Annals of Nuclear Medicine Vol. 17, No. 2, 153–157, 2003

Tc-99m-tetrofosmin scintigraphy in a primary giant cell tumor of bone with pulmonary metastases

Zeynep YAPAR,*[1] Mustafa KIBAR,*[1] Serdar OZBARLAS,*[2] Berksoy SAHIN,*[3]
Aysun UGUZ,*[4] Gulfiliz GONLUSEN*[4] and Mehmet Emin INAL*[5]

*Departments of *[1]Nuclear Medicine, *[2]Orthopedics, *[3]Oncology, *[4]Pathology and *[5]Radiology, Çukurova University Medical School, Adana, Turkey*

Giant cell tumor (GCT) is usually considered to be a benign entity. In rare cases, pulmonary metastases can be observed. This report documents the ^{99m}Tc-tetrofosmin scan findings of a conventional GCT of the femur and developed pulmonary nodules. The lung lesions were felt to be an example of benign metastases. According to our review, this is the first case in the literature demonstrating tetrofosmin accumulation in a GCT of bone and its pulmonary metastases.

Key words: Tc-99m-tetrofosmin, giant cell tumor of bone, pulmonary metastases

INTRODUCTION

GIANT CELL TUMOR of bone (GCT) is a locally osteolytic tumor with variable aggressiveness. These tumors encompass approximately 20% of all benign bone tumors. Despite being classified as benign, they can show aggressive behavior and metastasize in 1.9% to 9.5% of patients.[1–6] Most of the metastases are to the lung.[1–5]

^{99m}Tc-tetrofosmin (^{99m}Tc-1,2-bis [bis (2-ethoxyethyl) phosphino] ethane) is an agent developed for myocardial perfusion imaging.[7,8] It also has been shown to accumulate in viable tumor tissue, including nasopharyngeal,[9] breast,[10] lung cancer,[11] malignant thymoma,[12] medullary thyroid carcinoma,[13] musculoskeletal sarcoma[14] and brain tumors.[15]

CASE REPORT

A 36-year-old man had a history of curettage operation for a primary giant cell tumor at the lower end of the left femur. In microscopic examination of the curettage specimen, the basic pattern of the tumor was that of a moderately vascularized stroma with oval or plump, spindle-shaped mononuclear cells uniformly interspersed with multinucleated giant cells (Fig. 1A). The nuclei of stromal and giant cells were similar (Fig. 1B).

During the year following curettage, he had no complaint. One year later, he applied to the University Hospital with recurrent pain and swelling on prior operation site in April 2001. The patient presented to our department following plain radiographs of the left knee and chest.

The patient was examined scintigraphically using ^{99m}Tc-tetrofosmin (Myoview, Amersham International, Amersham, UK). The kit was prepared according to the manufacturer's instructions. Following intravenous injection of 555 MBq ^{99m}Tc-tetrofosmin, both femurs including knees were imaged from anterior projection with a large field of view gamma camera (Camstar, GE Medical Systems) equipped with a low-energy all-purpose collimator. Data were obtained every 2 second per 60 seconds for radionuclide angiography (128 × 128 matrix). Then Planar 5-min ^{99m}Tc-tetrofosmin images (256 × 256 matrix) were obtained for 30 min after radionuclide administration. Subsequently, whole-body and planar chest images were obtained.

Tetrofosmin images (Fig. 2) showed significantly increased both flow and uptake of 30 min tetrofosmin in the lower one-thirds of the left femur. On bilateral chest images, multiple pathologic tetrofosmin accumulation sites were seen throughout the lungs. Drawing background on the axillar region, quantitative analysis was also performed. For different foci shown on Figure 2D,

Received October 9, 2002, revision accepted December 26, 2002.

For reprint contact: Zeynep Yapar, M.D., Çukurova Üniversitesi Tıp Fakültesi, Nükleer Tıp Anabilim Dalı, Balcalı, Adana, TURKEY.

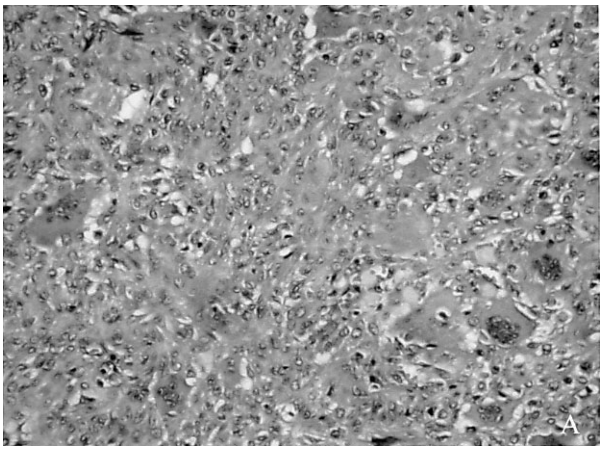

1A

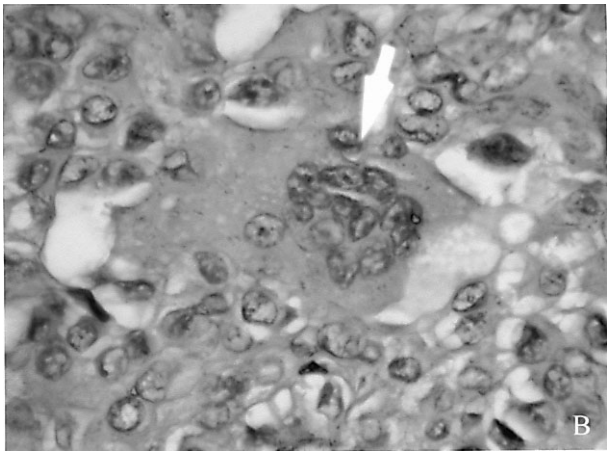

1B

Fig. 1 A: Oval or plump, spindle-shaped mononuclear cells uniformly interspersed with multinucleated giant cells with a moderately vascularized stroma are seen histopathologically. B: The nuclei of stromal and giant cells are similar.

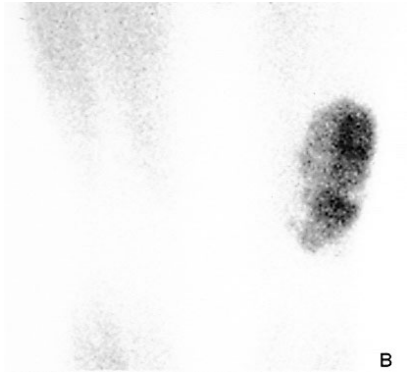

2B

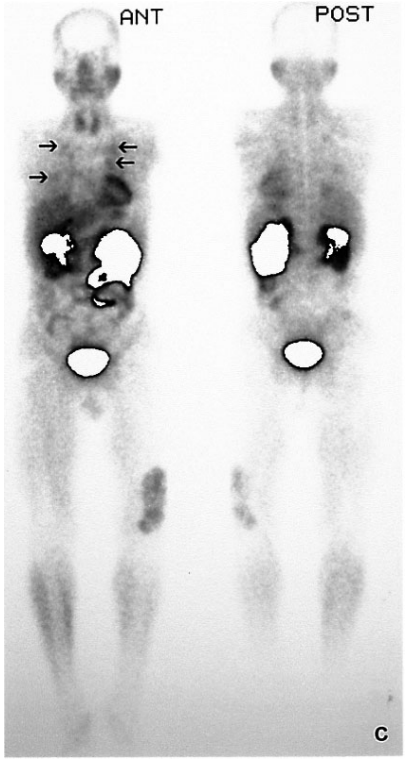

2C

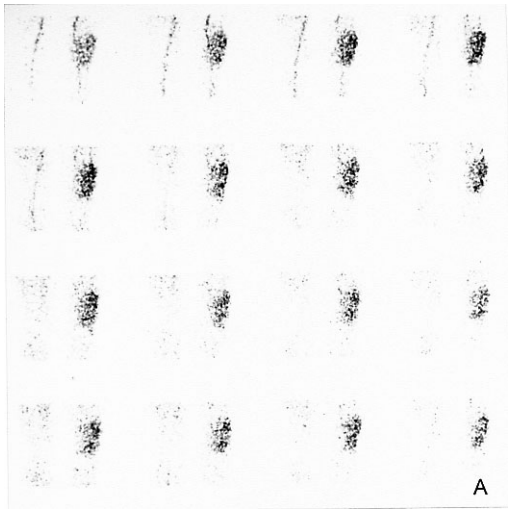

2A

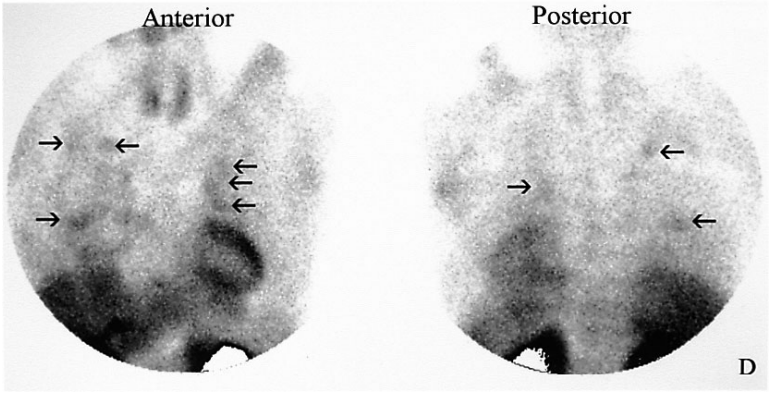

2D

Fig. 2 ^{99m}Tc-tetrofosmin scintigraphy before tumor excision. Radionuclide angiography (A) shows markedly increased tumor perfusion and also a significant ^{99m}Tc-tetrofosmin uptake in the tumor is seen on 30 min image (B). Planar chest (C) images demonstrate pathological tetrofosmin accumulation sites throughout both lungs, The uptake ratios of signed foci are changing in between 1.65 and 1.85, quantitatively.

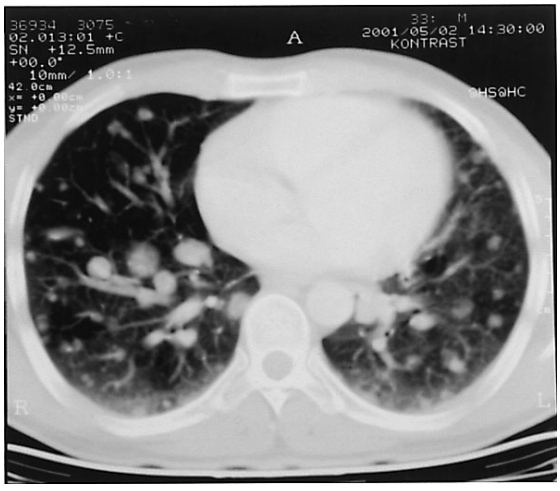

Fig. 3 CT images of the thorax before chemotherapy shows multiple bilaterally parenchymal infiltrative lesions especially at the right perihilar region.

the tumor/background ratios were calculated to be in the range of 1.65 and 1.85. Thorax CT images showed bilateral parenchymal infiltrative lesions concording with scintigraphic findings (Fig. 3).

On May 8, 2001, the tumor was excised and a tumor resection prosthesis was applied. Postoperative histologic evaluation was consistent with a giant cell tumor. For the systemic control of the disease, the patient received a combination consisted of high-dose methotrexate, cisplatin, doxorubicin, ifosfamide and mesna for 8 weeks.[16]

^{99m}Tc-tetrofosmin scintigraphy was again performed for pulmonary metastases to evaluate the response for

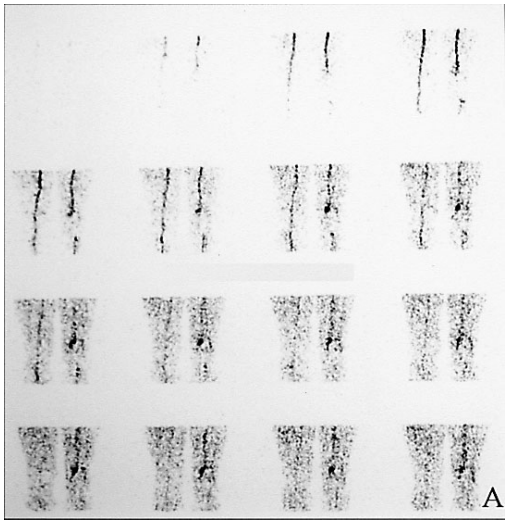

4A

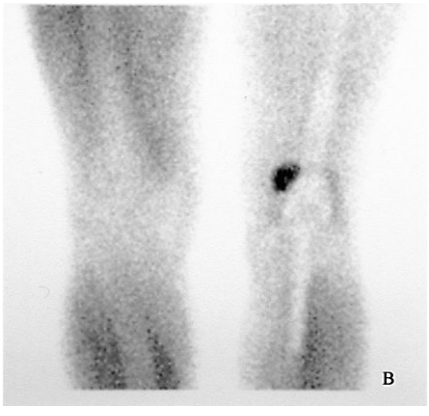

4B

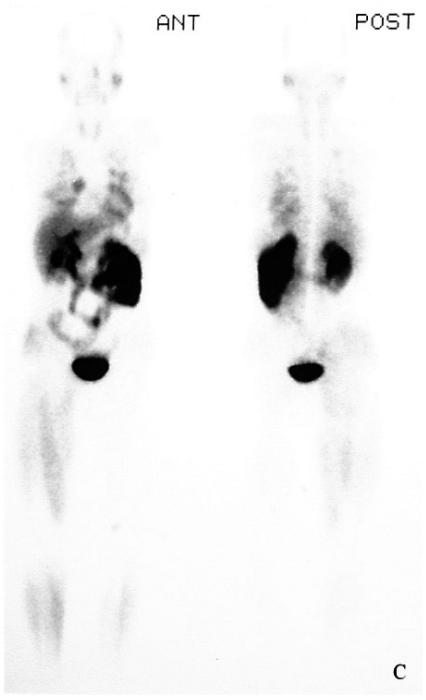

4C

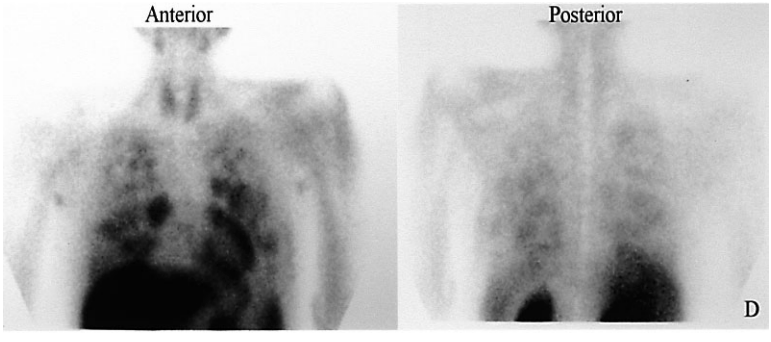

4D

Fig. 4 ^{99m}Tc-tetrofosmin scintigraphy repeated after surgery and chemotherapy. Radionuclide angiography (A) reveals markedly increased perfusion in the medial side of the knee prosthesis, the same region also shows intense tracer uptake (B). On chest (C) images, multiple pulmonary deposits which are more significant and extensive when compared to the previous study could easily be seen in both lungs. Quantitative analysis demonstrates the uptake ratios of different foci in the range of 2.57 and 3.0.

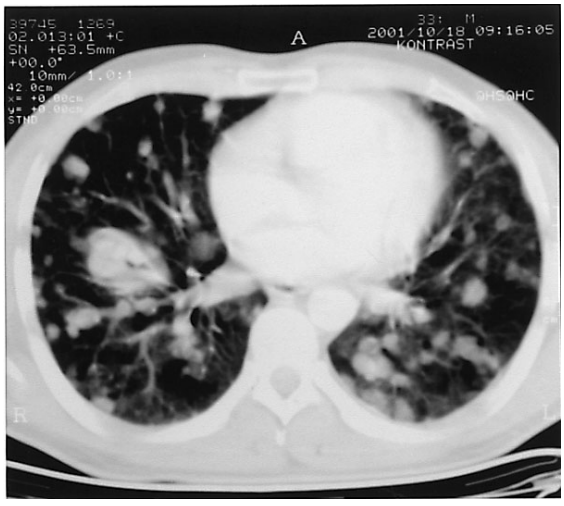

Fig. 5 On CT images of the thorax after chemotherapy, it is seen that the lesion seen at the right perihilar region shows expansion and multiple new lesions appear on both lungs.

chemotherapy in May, 2002. The same parameters were used for the second scintigraphy as described in the first one. The second scan revealed the pulmonary lesions more intense and extensive when compared to the previous one (Fig. 4). Quantitatively, the calculated uptake ratios of different foci against background were differing between 2.57 and 3, increased significantly when compared to the previous values. The second CT examination also confirmed the growth of the pulmonary metastases with expansion of the lesion at the right perihilar region in addition to the new lesions on both lungs (Fig. 5).

In the second tetrofosmin scintigraphy, a new small lesion with intense tetrofosmin uptake in the medial aspect of the knee prosthesis was also recognized (Fig. 4). Histopathological analysis could not be performed for this lesion, because the patient refused any surgical intervention.

The patient has been undertaking an investigational treatment regimen since 05-07-2002.

DISCUSSION

Although ^{99m}Tc-tetrofosmin uptake mechanism by tumor cells are not understood completely, the hypothesized mechanism directed the uptake on both cell membrane (Na/K^+ pump) and mitochondrial potentials.[17,18] Blood flow and metabolic status of cells determine the uptake. The main determinants are tissue characteristics, because retention of the tracer can occur if tumor cells are viable and metabolically active.[19] ^{99m}Tc-tetrofosmin imaging may thus act as an indicator of tumor aggressiveness by assessing the uptake of these tracers in tumors, and may be helpful in localizing the area of higher metabolism in the tumor. *In vitro* and *in vivo* studies revealed that ^{99m}Tc-tetrofosmin is efficient for the characterization of musculoskeletal sarcomas.[20,21] And also its accumulation in both malignant and benign musculoskeletal lesions has been shown to differ significantly.[22]

GCT of bone is a challenging clinicopathologic entity. Despite its benign designation, it has the capacity to recur locally and develop distant metastases.[1–7] Factors influencing the clinical course and biological aggression of GCT are unclear, Case reports in the literature describe metastatic lung nodules which demonstrate giant cell lesions with clearly benign histopathology.[23–25] However, there are reports in the literature showing malignant transformation of giant cell tumor,[26,27] and also its being malignant at onset.[28,29]

Scintigraphic experience in the evaluation for GCT of bone is extremely rare in the literature. In the report by Levine et al.,[30] either computed or conventional tomography was found to be superior over ^{99m}Tc-MDP bone scan in planning surgical margins of GCTs, and also in the same study gallium imaging revealed limited value in evaluating suspected GCT of bone because it did not show significant uptake in most of the tumors. In another report which examined the values of ^{99m}Tc(V)-DMSA and ^{67}Ga-citrate scans on three patients with tenosynovial GCTs, ^{99m}Tc(V)-DMSA scan was found to be useful in detecting tenosynovial GCT.[31] However, ^{67}Ga-citrate showed no accumulation in any of the tumors.

This report documents the utility of the ^{99m}Tc-tetrofosmin scintigraphy in the evaluation of a benign giant cell tumor of femur and indicates that the method may be useful in predicting chemotherapy response in the management of such patients. ^{99m}Tc-tetrofosmin scintigraphy detected not only the recurrent lesion and pulmonary metastases, but also showed the growth of the pulmonary nodules as a result of poor chemotherapy response in this ease.

REFERENCES

1. Liu P, Tao S, Xia K. Giant-cell tumor of bone: a review of diagnosis and treatment of 105 cases. *Zhonghua Zhong Liu Za Zhi* 1997; 19 (4): 313–315.
2. Tubbs WS, Brown LR, Beabout JW, Rock MG, Unni KK. Benign giant-cell tumor of bone with pulmonary metastases: clinical findings and radiologic appearance of metastases in 13 cases. *AJR Am J Roentgenol* 1992; 158 (2): 331–334.
3. Feigenberg SJ, Marcus RB, Zlotecki RA, Scarborough MT, Enneking WF. Whole-lung radiotherapy for giant cell tumors of bone with pulmonary metastases. *Clinical Orthopaedics and Related Research, Lippincott Williams & Wilkins* 2002; 401: 202–208.
4. Kay RM, Eckardt JJ, Seeger LL, Mirra JM, Hak DJ. Pulmonary metastasis of benign giant cell tumor of bone. Six histologically confirmed cases, including one of spontaneous regression. *Clin Orthop* 1994; 302: 219–230.
5. Takechi E, Ito S, Taguchi K. Follow-up study of giant cell tumor of bone. *Acta Med Okayama* 1982; 36 (5): 349–360.
6. Tyler W, Barrett T, Frassica F, McCarthy E. Skin metastasis

from conventional giant cell tumor of bone: conceptual significance. *Skeletal Radiol* 2002; 31 (3): 166–170.
7. Boomsma MM, Niemeyer MG, van der Wall EE, et al. Tc-99m tetrofosmin myocardial SPECT perfusion imaging: comparison of rest-stress and stress-rest protocols. *Int J Card Imaging* 1998; 14 (2): 105–111.
8. Grouters RG, Verzijlbergen JF, Muller AJ, et al. Prognostic value and quality of life in patients with normal rest thallium-201/stress technetium 99m-tetrofosmin dual-isotope myocardial SPECT. *J Nucl Cardiol* 2000; 7 (4): 333–341.
9. Kostakoglu L, Uysal U, Özyar E, et al. A comparative study of technetium-99m sestamibi and technetium-99m tetrofosmin single-photon emission tomography in the detection of nasopharyngeal carcinoma. *Eur J Nucl Med* 1997; 24: 621–628.
10. Obwegeser R, Berghammer P, Rodrigues M, et al. A head-to-head comparison between technetium-99m-tetrofosmin and technetium-99m-MIBI scintigraphy to evaluate suspicious breast lesions. *Eur J Nucl Med* 1999; 26: 1553–1559.
11. Takekawa H, Shinano H, Tsukamoto E, Koseki Y, Ikeno T, Miller F, et al. Technetium-99m-tetrofosmin imaging of lung cancer: relationship with histopathology. *Ann Nucl Med* 1999; 13 (2): 71–75.
12. Hashimoto T, Takahashi K, Goto M, et al. Detection of malignant thymoma in primary tumour and metastatic lesions using ^{99m}Tc-tetrofosmin scintigraphy. *Radiot Med* 2001; 19 (3): 169–172.
13. Adalet I, Kocak M, Oguz H, et al. Determination of medullary thyroid carcinoma metastases by ^{201}Tl, ^{99m}Tc(V)DMSA, ^{99m}Tc-MIBI and ^{99m}Tc-tetrofosmin. *Nucl Med Commun* 1999; 20 (4): 353–359.
14. Soderlund V, Jonsson C, Bauer HCF, et al. Comparison of technetium-99m-MIBI and technetium-99m-tetrofosmin uptake by musculoskeletal sarcomas. *J Nucl Med* 1997; 38: 682–686.
15. Soricelli A, Cuocolo A, Varrone A, et al. Technetium-99m-tetrofosmin uptake in brain tumours by SPECT: comparison with thallium-201 imaging. *J Nucl Med* 1998; 39: 802–806.
16. Picci P, Ferrari S, Bacci G, Gherlizzoni F. Treatment recommendations for osteosarcoma and adult soft tissue sarcomas. *Drugs* 1994; 47 (1): 82–92.
17. Arbab AS, Koizumi K, Toyama K, Araki T. Uptake of technetium-99m-tetrofosmin, technetium-99m-MIBI and thallium-201 in tumor cell lines. *J Nucl Med* 1996; 37: 1551–1556.
18. De Jong M, Bernard BF, Breeman WAP, et al. Comparison of uptake of ^{99m}Tc-MIBI, ^{99m}Tc-tetrofosmin and ^{99m}Tc-Q12 into human breast cancer cell lines. *Eur J Nucl Med* 1996; 23: 1361–1366.
19. Arbab AS, Koizumi K, Toyama K, Araki T. Ion transport systems in the uptake of ^{99m}Tc-tetrofosmin, ^{99m}Tc-MIBI and ^{201}Tl in a tumor cell line. *Nucl Med Commun* 1997; 18: 235–240.
20. Rodrigues M, Chehne F, Kalinowska W, et al. Comparative ^{99m}Tc-MIBI, ^{99m}Tc-tetrofosmin and ^{99m}Tc-furifosmin uptake in human soft tissue sarcoma cell lines. *Eur J Nucl Med* 2000; 27: 1839–1843.
21. Söderlund V, Jonsson C, Bauer HCF, et al. Comparison of technetium-99m-MIBI and technetium-99m-tetrofosmin uptake by musculoskeletal sarcomas. *J Nucl Med* 1997; 38: 682–686.
22. Yapar Z, Kibar M, Ozbarlas S, Uguz A, Zorludemir S. The value of Tc-99m-tetrofosmin scintigraphy as an indicator of malignancy amongst bone and soft-tissue tumors. *Eur J Nucl Med* 2001; 28 (8): 1236.
23. Cheng JC, Johnston JO. Giant cell tumor of bone, Prognosis and treatment of pulmonary metastases. *Clin Orthop* 1997; 338: 205–214.
24. van Hoeven KH, Kellogg K, Bavaria JE. Pulmonary metastasis from histologically benign giant cell tumor of bone. Report of a case diagnosed by fine needle aspiration cytology. *Acta Cytol* 1994; 38 (3): 410–414.
25. Obata H, Kido M, Kim ST, Nagata N, Yoshimatsu H. Multiple pulmonary metastasis from histologically benign giant cell tumor of the right radial olecranon. *Nihon Kyobu Shikkan Gakkai Zasshi* 1991; 29 (8): 1070–1074.
26. Mori Y, Tsuchiya H, Karita M, Nonomura A, Nojima T, Tomita K. Malignant transformation of a giant cell tumor 25 years after initial treatment. *Clin Orthop* 2000; 381: 185–191.
27. Marui T, Yamamoto T, Yoshihara H, Kurusaka M, Mizuno K, Akamatsu T. *De novo* malignant transformation of giant cell tumor of bone. *Skeletal Radiol* 2001; 30 (2): 104–108.
28. Merad M, Mesurolle B, Guinebretiere JM, Lecesne A, Missenard G, Vanel D. Recurrence of a primary malignant giant cell tumor of bone 14 years after initial surgery. *Eur Radiol* 2001; 11 (8): 1483–1486.
29. Mondal A, Kundu R, Chatterjee J. Primary malignant giant cell tumour of bone—a study of two cases with short review. *Indian J Pathol Microbiol* 2000; 43 (4): 403–407.
30. Levine E, De Smet AA, Neff JR, Martin NL. Scintigraphic evaluation of giant cell tumor of bone. *AJR Am J Roentgenol* 1984; 143 (2): 343–348.
31. Kobayashi H, Sakahara H, Hosono M, Shirato M, Konishi J, Kotoura Y, et al. Scintigraphic evaluation of tenosynovial giant-cell tumor using technetium-99m(V)-dimercaptosuccinic acid. *J Nucl Med* 1993; 34 (10): 1745–1747.